ELSEVIER

Polymer 41 (2000) 8425–8432

polymer

www.elsevier.nl/locate/polymer

Shear induced polymer migration: analysis of the evolution of concentration profiles

M. Criado-Sancho[a], D. Jou[b,c,*], L.F. Del Castillo[d], J. Casas-Vázquez[b]

[a]*Departamento de Ciencias y Técnicas Fisicoquímicas, UNED, Senda del Rey 9, 28040 Madrid, Spain*
[b]*Departament de Física, Universitat Autònoma de Barcelona, 08193 Bellaterra, Catalonia, Spain*
[c]*Institut d'Estudis Catalans, Carme 47, 08001 Barcelona, Catalonia, Spain*
[d]*Instituto de Investigaciones en Materiales, UNAM, Apartado Postal 70-360, Mexico DF, 04510, Mexico*

Received 22 November 1999; received in revised form 7 February 2000; accepted 2 March 2000

Abstract

In order to analyze the evolution of the concentration profile experimentally observed by MacDonald and Muller under shear-induced polymer migration in a rotating cone-and-plate device, we use a constitutive equation for the diffusion flux, where the gradient of a generalized non-equilibrium chemical potential appears instead of the concentration gradient. From this model of coupling between diffusion and viscous pressure, together with the mass balance equation, we derive some general features of the concentration profile, the temporal behavior of the polymer concentration near the apex of the cone and some relevant trends of the dynamical process of polymer migration.

Keywords: Polymer migration; Non-equilibrium chemical potential; Cone-and-plate

1. Introduction

In 1996, MacDonald and Muller [1] studied experimentally the shear-induced separation in a polymer solution in a rotating cone-and-plate configuration. They submitted some solutions of polystyrene of high molecular mass in oligomeric polystyrene to constant shear. The solutions were initially homogeneous, but, under the action of shear, the long polystyrene macromolecules were found to accumulate near the apex of the cone, thus exhibiting a coupling between viscous pressure and diffusion. Their main result was that the predictions of the constitutive equation for the flux of polymer $\boldsymbol{J}_2$

$$\boldsymbol{J}_2 = -D\nabla n - \frac{D}{RT}\nabla\cdot\mathbf{P}^{v} \tag{1}$$

with n the number of moles per unit volume, D the diffusion coefficient and $\mathbf{P}^{v}$ the viscous pressure tensor, yields for the rate of the mentioned separation process results that are two orders of magnitude lower than the experimental observations. This dramatic discrepancy makes their paper very interesting, as it is a challenge of our understanding of the couplings between diffusion and viscous pressure, a topic of much practical and theoretical interest [2–7], and which in Eq. (1) is described by the last term of the right-hand side.

In a recent paper [8], we showed that a drastic improvement of the results may be achieved when one uses instead of Eq. (1) a constitutive equation of the form

$$\boldsymbol{J}_2 = -\tilde{D}\nabla\mu_2 - \frac{D}{RT}\nabla\cdot\mathbf{P}^{v} \tag{2}$$

where μ_2 is the non-equilibrium chemical potential of the solute that depends in principle on non-equilibrium variables as for instance the viscous pressure itself in extended irreversible thermodynamics [9–15], or on the configuration tensor in other approaches. The coefficient $\tilde{D}$ is related to the classical diffusion coefficient D by $D = \tilde{D}(\partial\mu_2^{(eq)}/\partial n)$, where $\mu_2^{(eq)}$ is the local-equilibrium chemical potential of the solute. We will follow here, as in our previous paper [8], the thermodynamic framework of extended irreversible thermodynamics [9–15] because in this theory the non-equilibrium chemical potential depends directly on $\mathbf{P}^{v}$ and therefore the coupling between diffusion and viscous pressure through the first term on the right-hand side of Eq. (2) is described in the most direct way. Other theories, instead, [2–7] focus their interest on the purely dynamical coupling expressed by the second term of Eqs. (1) or (2) and pay little or no attention at all to the thermodynamic coupling coming

* Corresponding author. Tel.: +34-93-5811563; fax: +34-93-5812155.
E-mail address: jou@circe.uab.es (D. Jou).

0032-3861/00/$ - see front matter
PII: S0032-3861(00)00180-4

from the non-equilibrium chemical potential. Indeed, when the gradient of μ_2 is expressed in terms of the concentration gradient, the first term of Eq. (2) yields an effective diffusion coefficient introduced by comparing Eqs. (1) and (2)

$$D_{\text{eff}} = \tilde{D}(\partial\mu/\partial n) = D\Psi(n, \dot{\gamma}) \tag{3}$$

where the function Ψ is defined as

$$\Psi(n, \dot{\gamma}) = \frac{(\partial\mu/\partial n)}{(\partial\mu_{\text{eq}}/\partial n)} \tag{4}$$

depending on the concentration and the shear rate $\dot{\gamma}$.

In the conditions of the experiment by MacDonald and Muller [1] D_{eff} seems to be negative and two orders of magnitude higher than the classical diffusion coefficient [8], in qualitative agreement with the experimental conclusions. This improvement of the results makes it worth carefully considering the model [9–16] based on Eq. (2).

In Ref. [8] we showed that the sign and orders of magnitude of the effective diffusion coefficient obtained from Eq. (2) were consistent with experimental data, but we did not study the predictions of Eq. (2) on the evolution of the concentration profile. This analysis is the main original aim of the present paper. Another original aspect is that, in difference with Ref. [8], where we considered a solution of polystyrene in *trans*-decalin, here we consider the same solution studied by MacDonald and Muller, for which we lacked some data when Ref. [8] was written.

To study the evolution of the concentration profile, we undertake a simple mathematical analysis of some relevant features of the dynamical process of migration, in particular, the evolution of the polymer concentration near the apex of the cone, and the difference of concentration near the apex of the cone and near the edge of the system.

The plan of the paper is as follows. In Section 2 we discuss the general details of the model being used in this paper. In Section 3 we apply it to the system considered by MacDonald and Muller and derive some general features of the behavior of the concentration near the apex of the cone. Section 4 is devoted to the analysis of the concentration profile and of the behavior of the evolution of the concentration near the apex. Finally, we discuss the main results.

2. Basic features of the model

The essential difference between the transport Eqs. (1) and (2) is that in the first term of the latter the gradient of the chemical potential appears, whereas in the first term of the former there is the solute concentration. In extended irreversible thermodynamics, the chemical potential of a fluid under flow may depend not only on temperature, pressure and concentration, but also on the viscous pressure tensor (and maybe on other fluxes, as the heat flux and the diffusion flux). Therefore, the first term in Eq. (2) provides a coupling between diffusion and viscous pressure in addition to the more well-known coupling provided by the second term in Eqs. (1) and (2).

The form of Ψ follows from the first equality in Eq. (3) and from the relation mentioned above $\tilde{D} = D(\partial\mu_2^{(\text{eq})}/\partial n)^{-1}$. In our paper [8] we used for the equilibrium chemical potential of the polymer solutions under study, the expression from the classical Flory–Huggins model. The non-equilibrium chemical potential was obtained by differentiation of the Gibbs free energy expression in extended irreversible thermodynamics [6,16–18], namely

$$G(T, p, n_1, n_2, \mathbf{P}^{\text{v}}) = G_{\text{eq}}(T, p, n_1, n_2) + \frac{JV}{4T}\mathbf{P}^{\text{v}} : \mathbf{P}^{\text{v}} \tag{5}$$

where V is the volume of the system, n_i the number of moles of the component i and J the steady-state compliance ($J = \tau/\eta$, with η the shear viscosity and τ the relaxation time of the viscous pressure tensor). The chemical potential of species i is obtained from G by differentiation as

$$\mu_i = \left(\frac{\partial G}{\partial n_i}\right)_{T,p,\mathbf{P}^{\text{v}}} \tag{6}$$

To evaluate explicitly the non-equilibrium contribution to Eqs. (5) and (6) we use for J the formula following from the Rouse–Zimm model, namely

$$J = \frac{CM_2}{c\text{R}T}\left[1 - \frac{\eta_1}{\eta}\right]^2 \tag{7}$$

where C is the Rouse constant ($C = 0.4$), M_2 the molecular mass of the solute, η_1 the viscosity of the solvent, and c the polymer concentration expressed in mass of solute by unit volume. The Rouse–Zimm model is also used in Ref. [1], because the polymer concentrations used in the experiment are low, in such a way that the volume fraction occupied by the polymer is of the order of 10^{-7} and the entanglements are very unlikely.

In order to get a functional relation between viscosity and concentration, we take a linear approach to the usual Martin equation

$$\frac{\eta}{\eta_{\text{s}}} = 1 + [\eta]c + k[\eta]^2c^2 \tag{8}$$

k being the Huggins constant and $[\eta]$ the intrinsic viscosity.

The expression for the non-equilibrium contribution to the chemical potential of the solute is thus [8,18]

$$\frac{\mu_2^{(\text{ne})}}{\text{R}T} = \frac{Cv_1M_2[\eta]}{4\text{R}^2T^2}\mathbf{P}^{\text{v}} : \mathbf{P}^{\text{v}}\left\{\frac{M_2[\eta]}{v_1}\frac{\Phi(\tilde{c})}{\tilde{c}} + 2\left[\frac{M_2[\eta]}{\tilde{c}v_1} - m\right]\frac{P_5\tilde{c}}{P_6\tilde{c}}\right\} \tag{9}$$

where m is the ratio between the molar volumes of the solute and the solvent, v_1 the molar volume of the solvent, $\tilde{c}$ the reduced concentration defined by $\tilde{c} = [\eta]c$ (note that $\tilde{c}$ is related to n by means of $\tilde{c} = [\eta]nM_2$) and $\Phi(\tilde{c})$, $P_5(\tilde{c})$ and

Table 1
Physical properties of the solutions considered in the experiments in Ref. [1]

M_2 (kg mol^{-1})	Concentration (kg m^{-3})	Viscosity of the solution (Pa s)	Intrinsic viscosity (m^3 kg^{-1})
2000	2.14	165	0.122
4000	1.28	136	0.171
6850	0.963	120	0.233

$P_6(\tilde{c})$ the auxiliary functions defined as [8,17,18]

$$\Phi(\tilde{c}) = \tilde{c}\left[\frac{1+k\tilde{c}}{1+\tilde{c}+k\tilde{c}^2}\right]^2 \tag{10}$$

$$P_5(\tilde{c}) = (k-1)\tilde{c}^2 + (k^2-3k)\tilde{c}^3 - 3k^2\tilde{c}^4 - k^3\tilde{c}^5,$$
$$P_6(\tilde{c}) = (1+\tilde{c}+k\tilde{c}^2)^3 \tag{11}$$

When a cone-and-plate experiment is considered [1], we can write the expressions

$$\mathbf{P}^{\mathrm{v}} : \mathbf{P}^{\mathrm{v}} = (P^{\mathrm{v}}_{\phi\phi})^2 + 2(P^{\mathrm{v}}_{\phi\theta})^2 = \Xi(\dot{\gamma})\tilde{c}^2 \tag{12}$$

where ϕ and θ refer to the axial and azimuthal directions, respectively, and Ξ is given by

$$\Xi(\dot{\gamma}) = \left(\frac{RT}{M_2[\eta]}\right)^2 [4(\tau\dot{\gamma})^4 + 2(\tau\dot{\gamma})^2] \tag{13}$$

When Eqs. (12) and (13) are introduced in Eq. (9) the explicit expression for the derivative $(\partial\mu_2^{(\mathrm{ne})}/\partial\tilde{c})$ is given by

$$\frac{\partial\mu_2^{(\mathrm{ne})}}{\partial\tilde{c}} = \frac{Cv_1M_2[\eta]}{2RT}\Xi(\dot{\gamma})\left\{\frac{M_2[\eta]}{v_1}\Phi(\tilde{c}) + \left[\frac{M_2[\eta]}{v_1} - m\tilde{c}\right]\left[2\frac{P_5(\tilde{c})}{P_6(\tilde{c})} + \tilde{c}\frac{\mathrm{d}}{\mathrm{d}\tilde{c}}\left(\frac{P_5(\tilde{c})}{P_6(\tilde{c})}\right)\right]\right\} \tag{14}$$

The analysis of a specific system requires to introduce into Eq. (14) the numerical values for the material coefficients.

3. Application to the system studied by MacDonald and Muller

In the migration experiment carried out by MacDonald and Muller [1] the polymer solution confined in the cone-and-plate shear device has a homogeneous concentration ($\tilde{c}_0$ when it is expressed as a reduced one) before the system is sheared. As a consequence of coupling between diffusion and viscous pressure, a dependence of concentration on time and radial position is observed after the cone begins to rotate, yielding a concentration profile $\tilde{c}(r,t)$. This radial migration has two contributions: one of them is due to the second term in Eq. (2); this is the only contribution considered by MacDonald and Muller and yields a rather low separation. The second contribution, not considered in Ref. [1], is due to the dependence of μ on the viscous pressure, which makes possible that D_{eff} is negative and takes absolute values much higher than the classical diffusion D for concentration higher than a critical value $\tilde{c}_{\mathrm{c}}$. This additional contribution favors separation and accelerates the migration process very much. Since we are interested in the dynamical aspects of the migration process, we must look for the concentration range where $\Psi < 0$.

In Ref. [1] three solutions of polystyrene of high molecular mass solved in an oligomeric polystyrene of molecular mass 0.5 kg mol^{-1} and viscosity 80 Pa s were considered. Using the density of a polystyrene chain with 5000 segments reported by Wolf [19], the molar volume of a monomer unit can be estimated as 9.7×10^5 m^3 mol^{-1}, in such a way that the molar volume of the oligomeric solvent v_1 is equal to 4.66×10^4 m^3 mol^{-1}. Other properties of the solutions studied in Ref. [1] are collected in Table 1. It must be also noted that the relaxation times reported by MacDonald and Muller [1] were calculated from the Rouse model and this fact allows us to calculate the intrinsic viscosity values given in Table 1 and whose dependence on the molecular mass of the solute follows the expression

$$[\eta] = 2.25\times10^{-3}M_2^{0.524} \tag{15}$$

Concerning the Huggins constant k to be used in Eq. (8), the best value is obtained by fitting the experimental data of Table 1; this yields the result

$$k = 497.9M_2^{-0.49} \tag{16}$$

Whereas concentration in Ref. [1] is given by the weight fraction, in Table 1 the concentration is expressed by the mass of solute by unit volume c. In order to relate c with the weight fraction defined in the usual form

$$w_2 = \frac{n_2M_2}{n_1M_1 + n_2M_2} \tag{17}$$

where the subindices 1 and 2 correspond to the solvent and polymer, respectively, we will use the expression

$$c = \frac{M_1}{v_1}w_2 \cong \frac{M_0}{v_0}w_2 \tag{18}$$

M_0 and v_0 are the molecular mass and molar volume of a segment of polystyrene, and it is assumed that $M_2 = mM_1$ and $v_2 = mv_1$, where m may be calculated from the polymerization index of the solute.

Using the latter information, the numerical values of the chemical potential and its derivatives can be calculated for the system polystyrene solved in oligomeric polystyrene, and we obtain the results shown in Figs. 1 and 2 for the solution whose solvent has a molecular mass 2000 kg mol^{-1} (the system so called 2M in Ref. [1]). In Fig. 2 can be observed a critical concentration $\tilde{c}_{\mathrm{c}}$ for which the derivative of the non-equilibrium contribution to chemical potential is equal to zero for any shear rate considered. This concentration is the one corresponding to the maximum of the chemical potential in Fig. 1. When the calculations are carried out for several values of the polymer molecular mass, it is possible to reach the following fit $\tilde{c}_{\mathrm{c}} = 0.00545M^{0.199}$. Note that

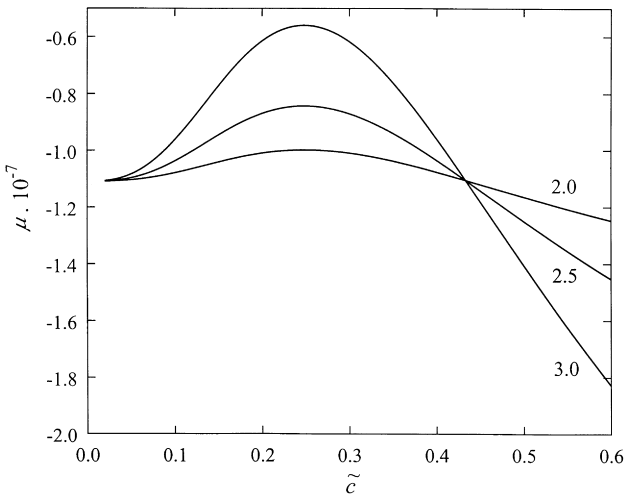

Fig. 1. The chemical potential of the solute for the system 2M of Ref. [1] obtained as the sum of the Flory–Huggins contribution and a non-equilibrium term (Eq. (9)). Each curve corresponds to the value of $\dot{\gamma}$ (in s^{-1}) which is indicated besides it; it is convenient to note that for the value of $\dot{\gamma}$ considered in this paper, the non-equilibrium contribution is more important than the Flory–Huggins one, and therefore, in agreement with Eq. (9), each value of $\dot{\gamma}$ is equivalent to introduce a vertical scale factor in the ordinate of the curves, without modifying their abscissa.

for the case 2M of Ref. [1] the initial value of the reduced concentration is 0.26, slightly above the critical value of the reduced concentration, which is 0.25. For values of $\tilde{c}$ higher than this critical value, D_{eff} defined in Eq. (3) is negative, and this enhances the separation process very much. In Ref. [8] we showed that the order of magnitude of this enhancement is compatible with the experimental results in Ref. [1].

It is interesting to remark that for increasing values of the shear rate, Fig. 1 is scaled vertically, i.e. the concentration corresponding to the maximum in Fig. 1 remains practically constant. This behavior is also seen in Fig. 2; this is due to the fact that the non-equilibrium contribution to the chemical potential is much higher and much more sensitive to concentration than the local-equilibrium chemical potential.

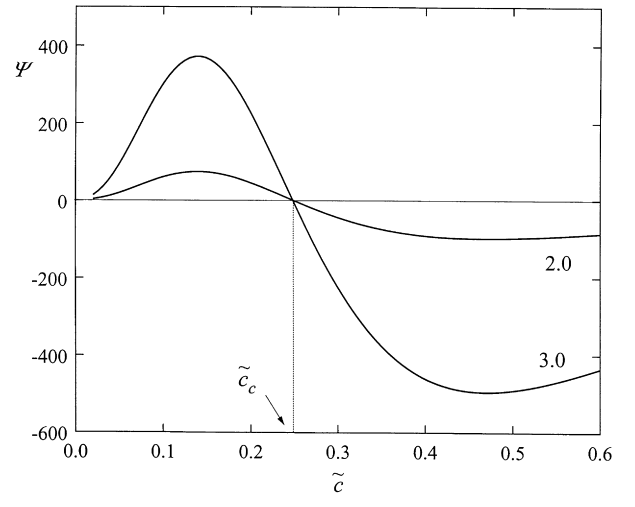

Fig. 2. The dependence of Ψ with respect to the composition of the system 2M in Ref. [1] Each curve corresponds to the value of $\dot{\gamma}$ (in s^{-1}) which is indicated besides it. According to Eq. (3), $\tilde{c}_c$ corresponds to a situation in which the effective diffusion coefficient D_{eff} in Eq. (3) vanishes. Therefore, for $\tilde{c} > \tilde{c}_c$ the separation process is enhanced. Note that the same argument presented in Fig. 1 leads us to identify $\tilde{c}_c$ with the abscissa of the maxima of Fig. 1.

In this paper we want to analyze in more detail some features of the results in Ref. [1]. To do that we will use Eq. (1), with the effective diffusion coefficient (Eq. (3)) instead of D, together with the mass balance equation to obtain the differential equation from which the shape of the concentration profile can be predicted

$$\frac{\partial \tilde{c}}{\partial t} = D\left[\frac{\partial \Psi}{\partial \tilde{c}}\left(\frac{\partial \tilde{c}}{\partial r}\right)^2 + \Psi\frac{\partial^2 \tilde{c}}{\partial r^2} + (2\Psi + \beta)\frac{1}{r}\frac{\partial \tilde{c}}{\partial r}\right] \tag{19}$$

where the new variable β is defined as $\beta = 2(\tau\dot{\gamma})^2$.

We assume for the solution of the latter equation a series expansion of the form

$$\tilde{c}(r,t) = \sum_{j=0} a_j(t) r^j \tag{20}$$

Since at the beginning of the experiment ($t = 0$) the concentration of the system is uniform, the following identifications can be established

$$a_0(0) = \tilde{c}_0 \qquad a_j(0) = 0 \ \ (j > 0). \tag{21}$$

while the concentration at the position $r = 0$ is given at any time by

$$\tilde{c}(0,t) = a_0(t) \tag{22}$$

After the results presented in Ref. [1] for the system 2M, it is possible to build Fig. 3 where the numerical values of $a_0(t)$ and its derivative are plotted as functions of time. From the plot of $a_0(t)$ we verify the existence of two values of the

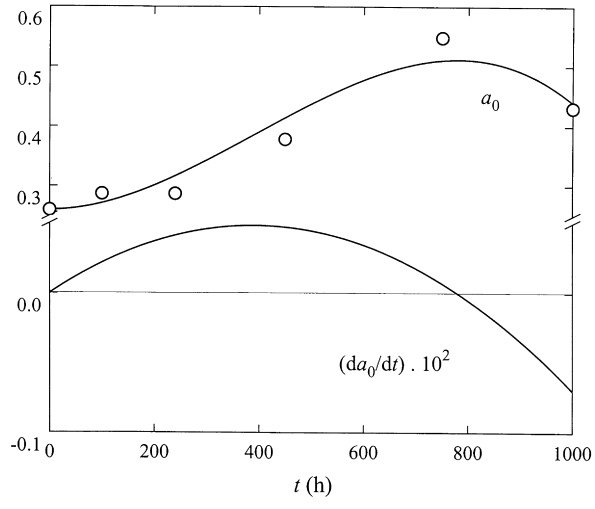

Fig. 3. The circles represent experimental values of the reduced concentration near the apex of the cone $\tilde{c}(0,t) = a_0$, measured in Ref. [1] for the system 2M submitted to a shear rate $\dot{\gamma} = 2\,s^{-1}$. The upper curve corresponds to a fit of such data, and the lower one to the corresponding derivative.

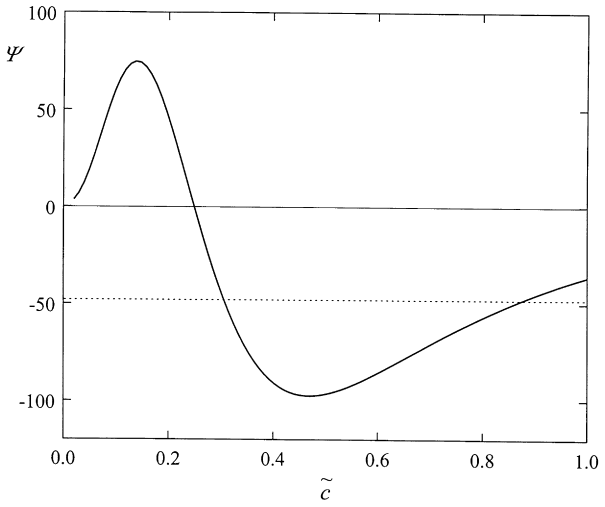

Fig. 4. The continuous curve corresponds to Ψ obtained for the system 2M of Ref. [1] at $\dot{\gamma} = 2\ s^{-1}$. The discontinuous line corresponds to $\Psi = -\beta/3$. Its intersection with the former curve corresponds to the values of abscissa 0.304 and 0.873 which, according to Eq. (28), correspond to the values of a_0 for which da_0/dt vanishes.

time for which the value of the derivative is zero: one of them corresponds to the beginning of the experiment and the other one is associated with a maximum for $a_0(t)$ at time $t > 0$. Note that the presence of this maximum prevents any monotone increase of concentration in the cone apex with the time. The presence of a maximum in the concentration near the apex agrees with the experimental findings of Ref. [1].

Taking into account Eqs. (20) and (21) it is easy to show the existence of the zero value for the derivative at $t = 0$. To prove the existence of the maximum we begin with the introduction in Eq. (19) of the auxiliary function Y defined by

$$\frac{Y(r,t)}{\Psi} = \frac{\partial \tilde{c}}{\partial r} \tag{23}$$

which allows us to write

$$\frac{\partial \tilde{c}}{\partial t} = D\left[\frac{\partial Y}{\partial \tilde{c}} + 2\frac{1}{r}Y + \beta\frac{1}{r}\frac{Y}{\Psi}\right] \tag{24}$$

Writing for Y, a series expansion as that previously introduced in Eq. (20)

$$Y(r,t) = \sum_{j=0} Y_j(t) r^j \tag{25}$$

its substitution in Eq. (19) lets us write the recurrence relations

$$\begin{cases} 0 = 2Y_0(t) + \beta a_1(t) \\ da_j/dt = D[(j+3)Y_{j+1}(t) + (j+2)\beta a_{j+2}(t)] \quad (j = 0, 1, \ldots) \end{cases} \tag{26}$$

When Eq. (23) is written for $r = 0$ and Eqs. (20), (25) and the first equation of the system (26) are taken into account, we get as a conclusion that $\Psi_0 = -\beta/2$, where Ψ_0 stands for $\Psi_0 = \Psi(a_0, \dot{\gamma})$. Since for a given shear rate Ψ_0 only depends on the concentration a_0, it is inferred that for a given shear rate the concentration in the apex of the cone, i.e a_0, would not depend on time, in contradiction with the experimental results of MacDonald and Muller (see their Fig. 7). In order to avoid this contradiction, while keeping the validity of Eq. (26), it must be proposed that $a_1(t)$ and $Y_0(t)$ are equal to zero for any time considered. If the derivative with respect to r is carried out in Eq. (20) and it is taken into account that $a_1 = 0$, we get the result

$$\left(\frac{\partial \tilde{c}}{\partial r}\right)_{r=0} = 0 \qquad \forall t \tag{27}$$

The differential Eq. (24) can be also particularized for $r = 0$, where it leads to the ordinary differential equation

$$\frac{da_0}{dt} = D[3\Psi_0 + \beta]\left(\frac{\partial^2 \tilde{c}}{\partial r^2}\right)_{r=0} \tag{28}$$

where the L'Hospital rule has been applied keeping in mind, as an additional hypothesis, than the second derivative of concentration with respect to position is a finite non-zero function. From Eq. (28) it is obvious that the maximum concentration corresponds to the value a_0 satisfying the equation $3\Psi(a_0, \dot{\gamma}) + \beta = 0$ which can be solved if an explicit expression for the chemical potential and its derivative are known.

When the system 2M is submitted to a shear rate $\dot{\gamma} = 2\ s^{-1}$ and τ is calculated from the value of intrinsic viscosity reported in Table 1 using the Rouse model, we get $\beta/3 = 48$. In Fig. 4 the values of $\Psi = -\beta/3 = -48$ are represented by a dotted line, in such a way that the concentrations a_0 for which the derivative da_0/dt vanishes are 0.304 and 0.873. We see, therefore that there appear two different values instead of the only experimental value $a_0 = 0.55$ observed in Fig. 3. A possible way to overcome this problem could be to adjust some parameter of the model (for instance, the Huggins constant) in such a way that the dotted line in Fig. 4 intersects this curve in the minimum.

4. On the concentration profile

From what we have said above, it is possible to obtain several conditions which must be verified by the concentration profiles reported in Ref. [1], namely

$$\left(\frac{\partial \tilde{c}}{\partial r}\right)_{r=0} = 0 \qquad \forall t \tag{29}$$

$$\tilde{c}(0,t) = a_0(t) \ \ \forall t \qquad \tilde{c}(r,0) = \tilde{c}_0 \ \ \forall r \tag{30}$$

$$\left(\frac{\partial^2 \tilde{c}}{\partial r^2}\right)_{r=0} \neq 0 \tag{31}$$

As a consequence, the concentration profile must show a

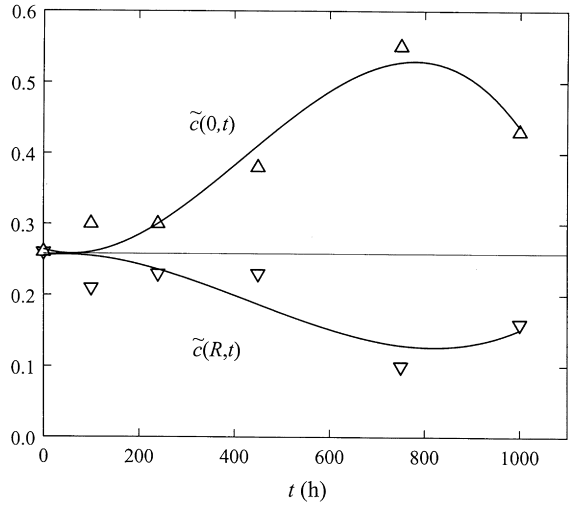

Fig. 5. The up triangles indicate the experimental values of the concentration near the apex of the cone for the system 2M of Ref. [1] submitted to a shear rate $\dot{\gamma} = 2\ s^{-1}$ for different values of time. The down triangles represent the concentration near the edge of the cylinder. The curves are the corresponding fits to each set of values of concentration.

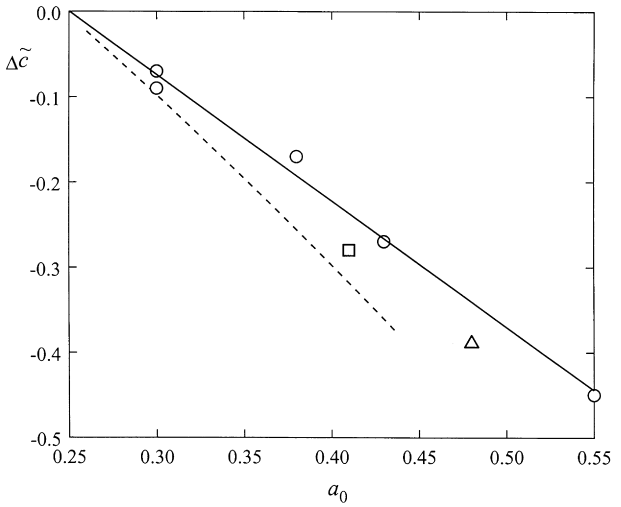

Fig. 6. Representation of the values of $\Delta\tilde{c}(R,t)$ at a given time as a function of a_0 at the same instant of time. The circles correspond to the experimental values measured in Ref. [1] for the system 2M submitted to $\dot{\gamma} = 2\ s^{-1}$, the triangles to the values obtained at $\dot{\gamma} = 3\ s^{-1}$ and the square corresponds to $\dot{\gamma} = 1.2\ s^{-1}$. The continuous line is the fit corresponding to the values with $\dot{\gamma} = 2\ s^{-1}$. The dashed curve has been calculated in a theoretical way, assuming hypothesis (39).

functional structure of the form

$$\tilde{c}(r,t) = a_0(t) + \alpha_1(t) r^n Z(r,t) \tag{32}$$

in such a way that by calculation of its first two derivatives with respect to the radius, and by taking into account conditions (29) and (30) it may be concluded that the parameter n must be equal or higher than 2. If we focus our attention on the concentration profiles measured by MacDonald and Muller (see their Figs. 7 and 8) we may introduce the new variable

$$\Delta\tilde{c}(r,t) = \tilde{c}(r,t) - \tilde{c}(0,t) \tag{33}$$

which satisfies the condition

$$\lim_{r\to\infty} \Delta\tilde{c}(r,t) = \xi(t) \tag{34}$$

The experimental information about $\tilde{c}(r,t), \tilde{c}(0,t)$ and $\tilde{c}(R,t)$ is summarized in Figs. 5 and 6.

One of the possible options in order that Eqs. (32) and (34) are compatible, is that the function $Z(r,t)$ in Eq. (32) is the inverse of a polynomial of second degree in r, in such a way that the concentration profile follows a functional expression of the form

$$\tilde{c}(r,t) = a_0(t) + \alpha_1(t) \frac{r^2}{\beta_0(t) + \beta_1(t) r + \beta_2(t) r^2} \tag{35}$$

which for the sake of simplicity may be written in the less general, but simpler form

$$\tilde{c}(r,t) = a_0(t) + \frac{\alpha(t) r^2}{1 + \beta_2(t) r^2}. \tag{36}$$

5. Analysis of the concentration at the apex as a function of time

When Eq. (36) is substituted into Eq. (28) one gets the new differential equation

$$\frac{da_0}{dt} = 2D[3\Psi_0 + \beta]\alpha \tag{37}$$

The fact that a_0 as well as da_0/dt are functions of time, may be given a geometric interpretation by considering that we have the parametric equations of a curve in a Cartesian coordinate system of coordinates given by a_0 and da_0/dt. Therefore, if one uses the curves of Fig. 3 to find the values of a_0 and da_0/dt at any value of t, it is possible to plot Fig. 7, which visualizes the interval of values of a_0 for which da_0/dt is a univocal function of a_0 and, recalling that $\Psi_0 = \Psi(a_0, \dot{\gamma})$, it is inferred from Eq. (37) that for this interval of concentration there must exist a functional relation of the kind $\alpha(a_0)$. This result allows us to go from the differential Eq. (37) to the following integral:

$$\frac{1}{2D} \int_{a_0^*}^{a_0} \frac{dx}{[3\Psi(x) + \beta]\alpha(x)} = t - t^* \tag{38}$$

where the superindex * refers to the point in the concentration–time plane for which the solution passes.

5.1. Additional hypothesis for the evaluation of the concentration profile

The first difficulty found in the integration of Eq. (38) is that we ignore the explicit dependence $\alpha(a_0)$, and therefore,

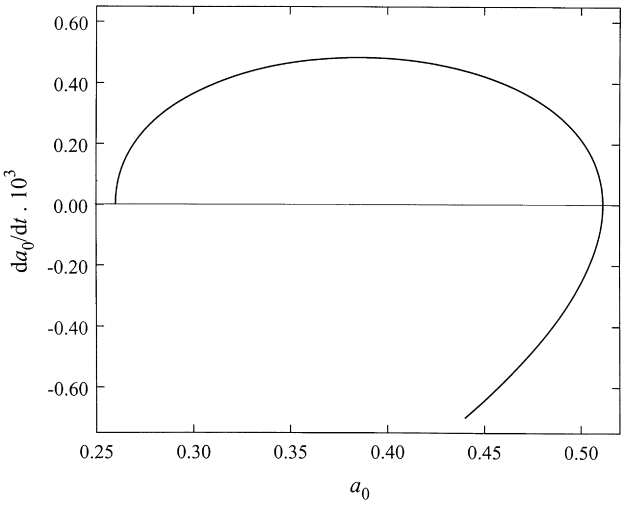

Fig. 7. When the parameter t is eliminated from the two curves of Fig. 3, there exists a range of values of a_0 for which it is possible to express da_0/dt as a function of concentration a_0.

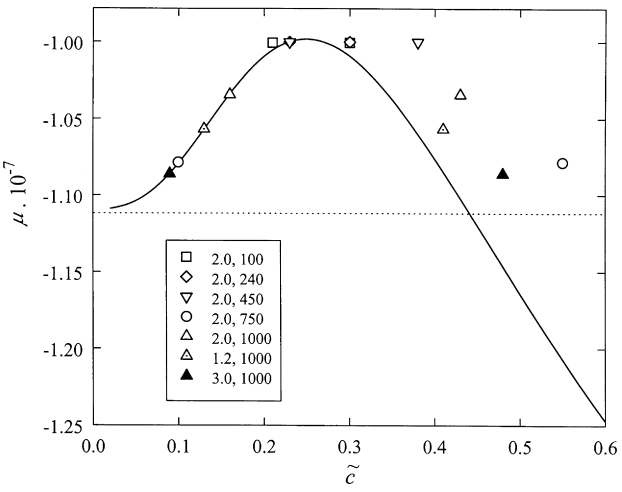

Fig. 8. The curve corresponds to the chemical potential used in this paper for the system 2M of Ref. [1]. The symbols correspond to the experimental values of Ref. [1] for several values of $\dot{\gamma}$ and time. The dots corresponding to $\tilde{c}(R,t)$ have been drawn on the curve, and the corresponding values for $\tilde{c}(0,t)$ have been represented on the horizontal line, which crosses its homologous point $\tilde{c}(R,t)$.

it is necessary to look for new hypotheses that allow us to determine such a functional dependence.

If the experimental values of $\Delta\tilde{c}(R,t)$ are plotted as a function of the concentration in the apex of the cone $a_0(t)$, a practically linear relation is obtained, which is shown in Fig. 6. It is rather remarkable that this line is practically independent of the value of the shear rate, at least in the range of values of shear rate considered in Ref. [1].

On the other side, if the experimental values of the concentration at the edge of the cylinder $\tilde{c}(R,t)$ for different values of time are represented on the curve $\mu(\tilde{c})$, derived theoretically from our model (using Eq. (9) and the Flory–Huggins theory), and the experimental values of $\tilde{c}(0,t)$ are plotted on the same horizontal, Fig. 8 is obtained. The observations in Fig. 8 may be roughly justified by introducing the hypothesis

$$\mu[\tilde{c}(0,t)] = \mu[\tilde{c}(\infty,t)] \tag{39}$$

This would be exact in equilibrium, but is only approximate for non-equilibrium steady states. The first restriction of this approximation is the fact that its range of validity is necessarily less than the value of the concentration for which the curve $\mu(\tilde{c})$ and the dotted curve represented in Fig. 8 intersect each other. This implies that the maximum value of the reduced concentration that we may safely consider in the present range of approximations is approximately 0.43 (this value will be denoted $\tilde{c}_{\lim}$), in contrast with the maximum value 0.55 derived from Fig. 3.

It is convenient to mention that when the shear rate increases, the equilibrium contribution to the chemical potential becomes less and less important, in such a way that an increase of $\dot{\gamma}$ only implies a multiplicative vertical scale factor $\mu(\tilde{c})$ (see Fig. 1). Therefore, if the bold hypothesis (39) is accepted, it follows that the values of $\Delta\tilde{c}(R,t)$ in Fig. 6, obtained theoretically from it (discontinuous line) will be practically unaffected by the shear rate. This is experimentally confirmed in the range of values of $\dot{\gamma}$ between 2 and 3 s^{-1} that we have considered in this paper.

5.2. Some calculation details

The main steps we propose in order to determine a concentration profile are the following ones:

(i) Given a value of a_0 we determine which value of the concentration satisfies the condition (39). In this way, we obtain the theoretical value for $\Delta\tilde{c}$ which is represented by the discontinuous line in Fig. 6.
(ii) From Eq. (36) it is possible to write $\beta_2 = \alpha/\Delta\tilde{c}_\infty$, in such a way that only an unknown parameter appears in the equation for the concentration profile (Eq. (36)).
(iii) We carry out a material balance along the radial coordinate. To do that we decompose the volume V in a series of N volume elements V_i and we apply the condition of mass conservation expressed as

$$\sum_{i=1}^{N} \tilde{c}_i V_i = \tilde{c}_0 V \tag{40}$$

This constitutes a functional relation of the form $f(a_0,\alpha) = 0$, which defines the function $\alpha = \alpha(a_0)$. The algorithm we have just described yields the concentration profile shown in Fig. 9. Note that the solution of the differential Eq. (37) through the point (t^*, a_0^*) can be obtained accomplishing a numerical integration of Eq. (38), assuming that the value of the coefficient D is known.

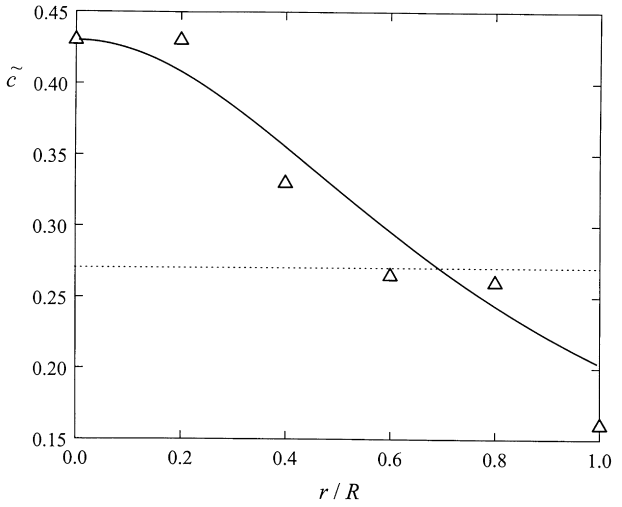

Fig. 9. The concentration profile calculated by following the algorithm presented in Section 5.2 of this paper when the value $a_0 = 0.43$ is assumed. The experimental values correspond to the system 2M of Ref. [1] submitted to a shear rate $\dot{\gamma} = 2\ s^{-1}$ during 1000 h.

6. Concluding remarks

We have studied several general features of the shear-induced polymer separation in a cone-and-plate situation considered experimentally in Ref. [1]. As shown in Ref. [1], the transport Eq. (1) is not satisfactory, because it gives a separation too slow. In contrast, it was seen in Ref. [8] that the use of the generalized chemical potential of EIT in Eq. (2) yields a much faster separation, because the effective diffusion coefficient becomes negative for concentrations higher than a critical one.

In Ref. [8], our attention was focused on the effective diffusion coefficient. Here, we take a more detailed dynamical analysis, by assuming a series expansion for the concentration profile.

The most interesting results are, in our opinion, the following ones:

(a) The nonmonotonic temporal behavior of the polymer concentration near the apex of the cone, which exhibits an overshoot behavior, which reaches a maximum higher than the final steady value; this is observed experimentally and follows from the consistency arguments here. Analogously, the concentration near the edge of the cylinder exhibits a negative overshoot, i.e. it reaches a minimum lower than the final steady concentration.

(b) For the range of values of the dimensionless shear rate studied here, the difference of concentrations near the apex and near the edge of the cone as a function of the latter concentration is practically linear (see Fig. 6) and this line is practically independent of the shear rate.

It could also be argued whether anisotropic effects could be sufficiently well described by the form Eq. (5) of the Gibbs free energy. In Ref. [20] we have considered the influence of anisotropy terms in Gibbs free energy, as described by the higher-order coupling of the form $\boldsymbol{J}\cdot\mathbf{P}^{\nu}\cdot\boldsymbol{J}$, on the spinodal line of solutions under shear; the influence of such terms turned out to be of the order of 5% of the influence of the second-order terms $P^{\nu} : P^{\nu}$, and therefore, we do not consider them here. A different, and open topic is the possible anisotropy in the diffusion tensor, which is beyond the purely thermodynamic analysis.

Acknowledgements

This work has been partially supported by the Dirección General de Asuntos del Personal Académico of UNAM, México under grant IN-106797. MC-S, DJ and JC-V also acknowledge the partial support of the Dirección General de Enseñanza Superior e Investigación Científica of the Spanish Ministry of Education under grant PB94-0718.

References

[1] MacDonald MJ, Muller SJ. J Rheol 1996;40:259.
[2] Agarwal US, Dutta A, Mashelkar RA. Chem Engng Sci 1994;49:1693.
[3] Beris AN, Mavranzas VG. J Rheol 1994;38:1235.
[4] Ottinger HC. Rheol Acta 1992;31:14.
[5] Onuki A. Phys Rev Lett 1989;62:2472.
[6] Milner ST. Phys Rev E 1993;48:3674.
[7] Helfand D, Fredickson GH. Phys Rev Lett 1989;62:2458.
[8] Del Castillo LF, Criado-Sancho M, Jou D. Polymer 2000;41:2633.
[9] Jou D, Casas-Vázquez J, Lebon G. Rep Prog Phys 1988;51:1105.
[10] Jou D, Casas-Vázquez J, Lebon G. Rep Prog Phys 1999;62:1035.
[11] Jou D, Casas-Vázquez J, Lebon G. Extended irreversible thermodynamics 2. Berlin: Springer, 1996.
[12] Nettleton RE, Sobolev SL. J Non-Equilib Thermodyn 1995;20:205.
[13] Nettleton RE, Sobolev SL. J Non-Equilib Thermodyn 1995;20:297.
[14] Nettleton RE, Sobolev SL. J Non-Equilib Thermodyn 1996;21:1.
[15] García-Colín LS, Uribe FJ. J Non-Equilib Thermodyn 1991;16:89.
[16] Jou D, Casas-Vázquez J, Criado-Sancho M. Adv Polym Sci 1995;120:207.
[17] Jou D, Casas-Vázquez J, Criado-Sancho M. Thermodynamics of fluids under flow. Berlin: Springer, 2000 (in press).
[18] Criado-Sancho M, Jou D, Casas-Vázquez J. Polymer 1995;6:4107.
[19] Wolf BA. Macromolecules 1984;17:615.
[20] Criado-Sancho M, Jou D, Casas-Vázquez J. Physica A 1999;274:466.